The 2004 North Slope of Alaska Arctic Winter Radiometric Experiment: Overview and Recent Results

E.R. Westwater, D. Cimini, M. Klein, and V. Leuski
Cooperative Institute for Research in Environmental Sciences
University of Colorado/National Oceanic and Atmospheric Administration – Earth System Research
Boulder, Colorado

V. Mattioli
Dipartimento di Ingegneria Elettronica e dell'Informazione
Università di Perugia
Perugia, Italy

A.J. Gasiewski
Department of Electrical and Computer Engineering
University of Colorado
Boulder, Colorado

J.C. Liljegren
Department of Energy – Argonne National Laboratory
Argonne, Illinois

Introduction

Accurate measurements of water vapor in the Arctic winter, either in situ or remote, are difficult to achieve. These measurements are important to studies in infrared radiative transfer. To focus on measurements during cold temperatures (< - 20ºC) and low amounts of vapor (Precipitable Water Vapor, 5 mm), an Intensive Operating Period (IOP) was conducted at the U.S. Department of Energy's Atmospheric Radiation Measurement (ARM) Program's field site near Barrow, Alaska, during March 9 to April 9 2004. In this paper we give an overview of the experiment and show some highlights of the data analysis. Other results from this experiment are provided in [1, 2]. The major goal was to demonstrate that millimeter wavelength radiometers can substantially improve water vapor observations during the Arctic winter. Secondary goals included forward-model studies over a broad frequency range, demonstration of recently developed calibration techniques, the comparison of several types of in situ water vapor sensors, and the application of infrared imaging techniques. During this IOP, radiometers were deployed over a broad frequency range (22.235 to 400 GHz), including several channels near the strong water vapor absorption lines at 183.31 and 380.2 GHz. These radiometers were

supplemented by frequent radiosonde observations and other in situ observations, including several "Snow White" Chilled Mirror radiosondes. The radiometers deployed are also useful for measuring clouds during these cold conditions. Instruments that were deployed include the Ground-based Scanning Radiometer (GSR) of National Oceanic and Atmospheric Administration (NOAA) Earth System Research Laboratory, the microwave radiometer (MWR) and the Radiometric Profiler of ARM, a Global Positioning System operated by NOAA Earth System Research Laboratory. In addition, all of the ARM active cloud sensors (Millimeter Wave Cloud Radar and lidars) were operating. A list of the instruments that were deployed is shown in Table 1.

Table 1. Instruments Deployed and Parameters Derived during the 2004 North Slope of Alaska (NSA) Arctic Winter Radiometric Experiment. PWV = Precipitable Water Vapor. LWP = Liquid Water Path. T(z) = temperature profile.

Instrument	Frequencies (GHz)	Parameters
ARM Microwave Radiometer (MWR)	23.8, 31.4	PWV, LWP
NOAA Ground-based Scanning Radiometer (GSR)	50.300, 51.760, 52.625, 53.290, 53.845, 54.400, 54.950, 55.520, 56.025, 56.215, 56.325	T(z), LWP
ARM Microwave Radiometer Profiler (MWRP)	22.235, 23.035, 23.835, 26.235, 30.000, 51.250, 52.280, 53.850, 54.940, 56.660, 57.290, 58.800	PWV, LWP, T(z)
NOAA GSR	89 (H & V)	LWP
NOAA GSR	$183.31 \pm (0.55, \pm 1.0, \pm 3.05, \pm 4.7, \pm 7.0, \pm 12.0, \pm 16.0$	PWV
NOAA GSR	340 (H & V)	LWP
NOAA GSR	$380.197 \pm (4.0, \pm 9.0, \pm 17.0)$	PWV
UMontana Infrared Cloud Imager (ICI)	8 – 14 μm	Cloud Images
NOAA GSR	10 μm	Cloud
NOAA GPS		PWV

Radiometric Data

During the month long experiment a large range of conditions were encountered, both in temperature, water vapor, and clouds. From Figure 1, we see that the temperature ranged from -40ºC to 0ºC, the Precipitable Water Vapor PWV from about 0.8 mm to 15 mm, and that significant amounts of both liquid (Liquid Water Path- LWP), and ice clouds (Ice Water Path-IWP) were encountered. The overall integrated moisture statistics for the 30-day experiment are shown in Figure 2. In particular, we obtained a good variety of clear and cloudy conditions. This range in meteorological conditions was also reflected in the multi-frequency brightness temperatures (Tb's) observed by the GSR (see Figure 3). Note the substantially increased sensitivity by the GSR to both water vapor and clouds relative to the MWR. In this figure and in general, we used the threshold infrared brightness temperature Tir of 223.2 K as a cloud indicator, and any infrared Tb greater that this value was labeled as containing clouds.
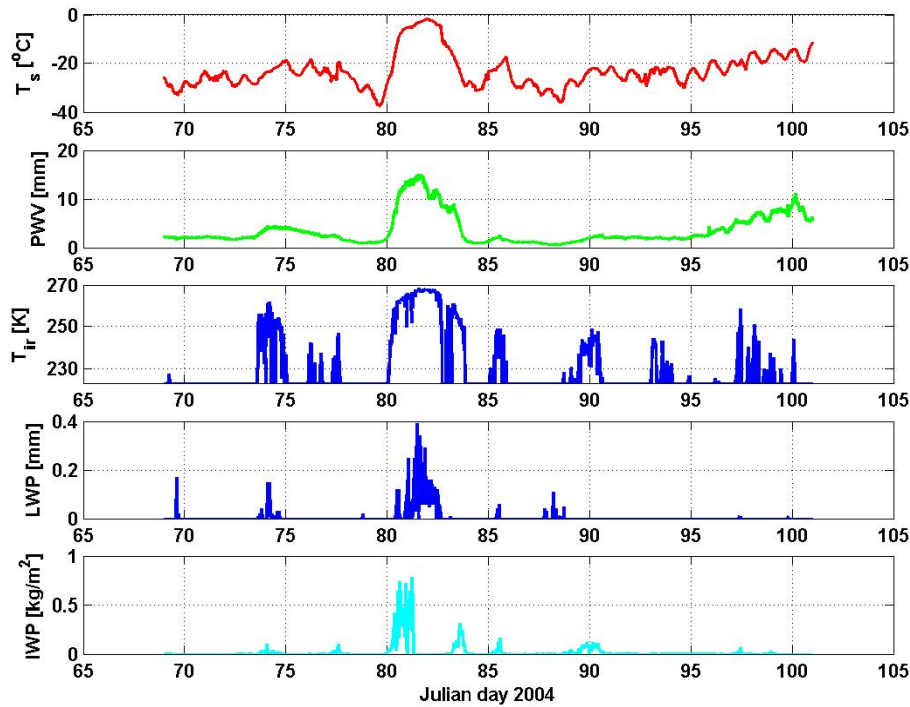
Figure 1. Time series of observed meteorological parameters during the NSA 2004 IOP. The PWV and LWP were observed by the ARM MWR, the Infrared temperature by the ARM MWRP, and the ICL by the ARM Millimeter Wave Cloud Radar.
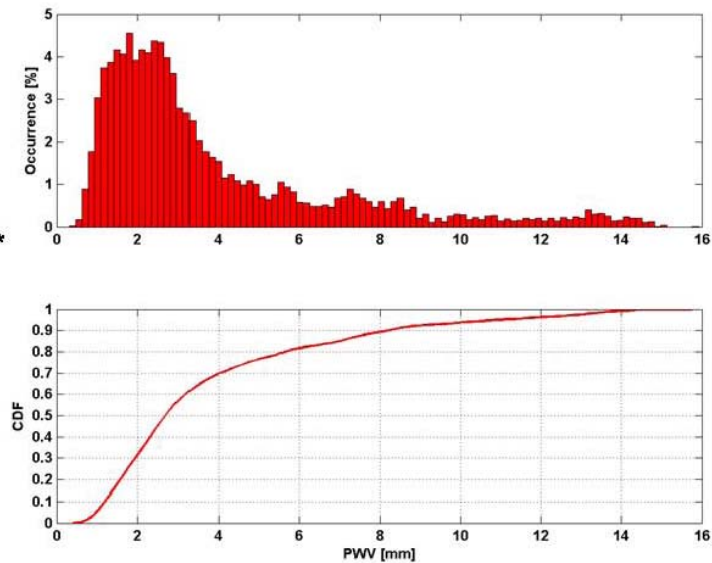
Figure 2. Data base integrated moisture statistics for the 30-day NSA IOP. The clear statistics were based on MWRP Tir and PWV. Cloud statistics based on the MWR LWP * and the mixed phase, pure liquid, and ice based on Microwave Radiometer Profiler (MWRP) LWP and MMCR IWP and MMCR IWP [10].
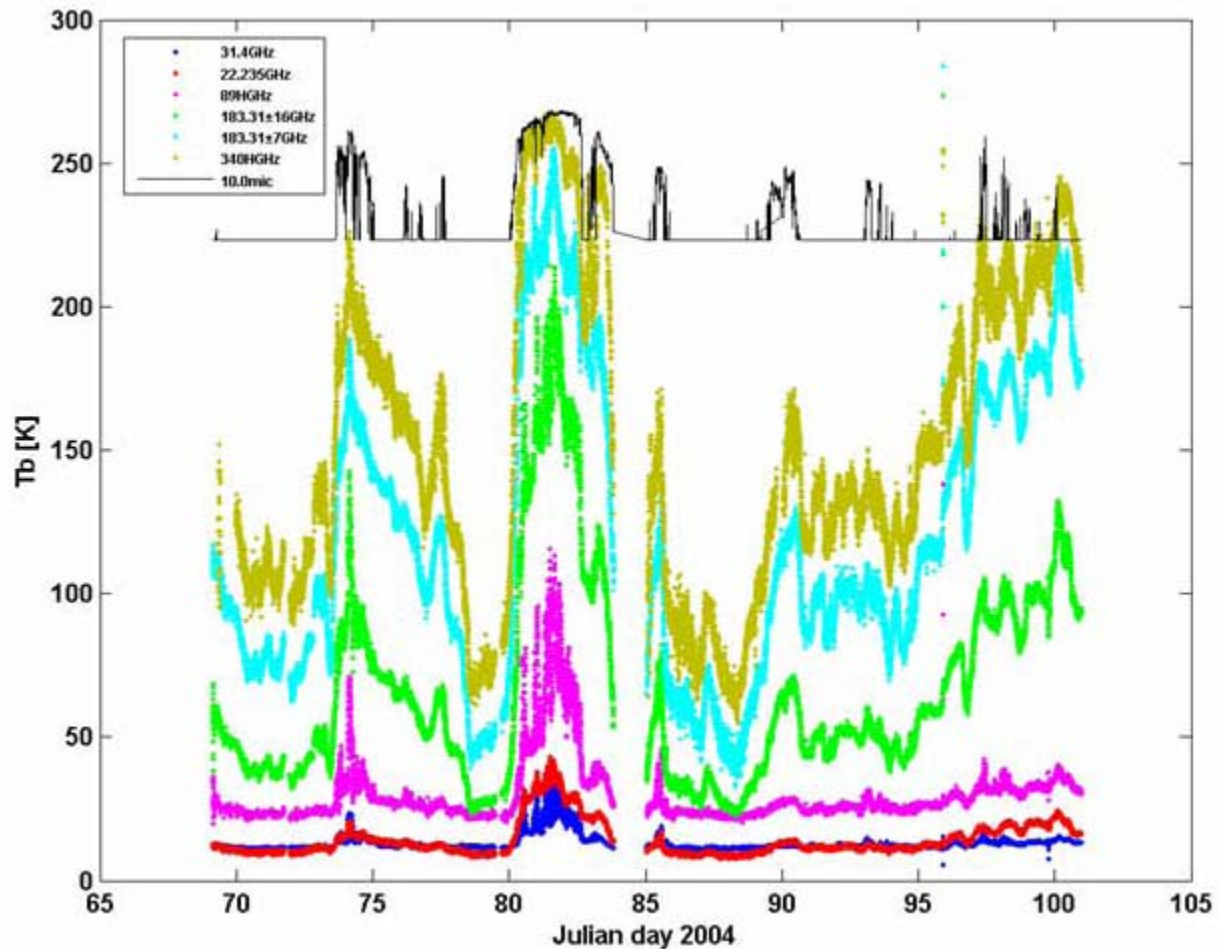
Figure 3. Time series of observed GSR Tbs during the NSA 2004 IOP. In this figure, only the most transparent of the GSR channels are shown.

Using data such as these, we can compare the sensitivities of the various channels to water vapor and cloud liquid. Since we do not have a completely reliable measure of PWV and LWP for all conditions we have chosen the retrievals from the MWR as our standard of comparison. From these data, the relative sensitivities of the various channels to both vapor and liquid can be obtained, following the method outlined in [2]. The results for PWV are shown in Figure 4A. It is clear from this figure that the sensitivity of even the more transparent GSR channels is not a linear function of PWV. We also derived the sensitivity of GSR channels as a function of LPW, using the method shown in [2] to remove the effects of PWV (see Figure 4B). It apparent from the slopes of the lines for the 89 and the 183.31 ±16 GHz channels that enhanced sensitivities to LWP relative to 23.8 and 30.0 GHz are present.
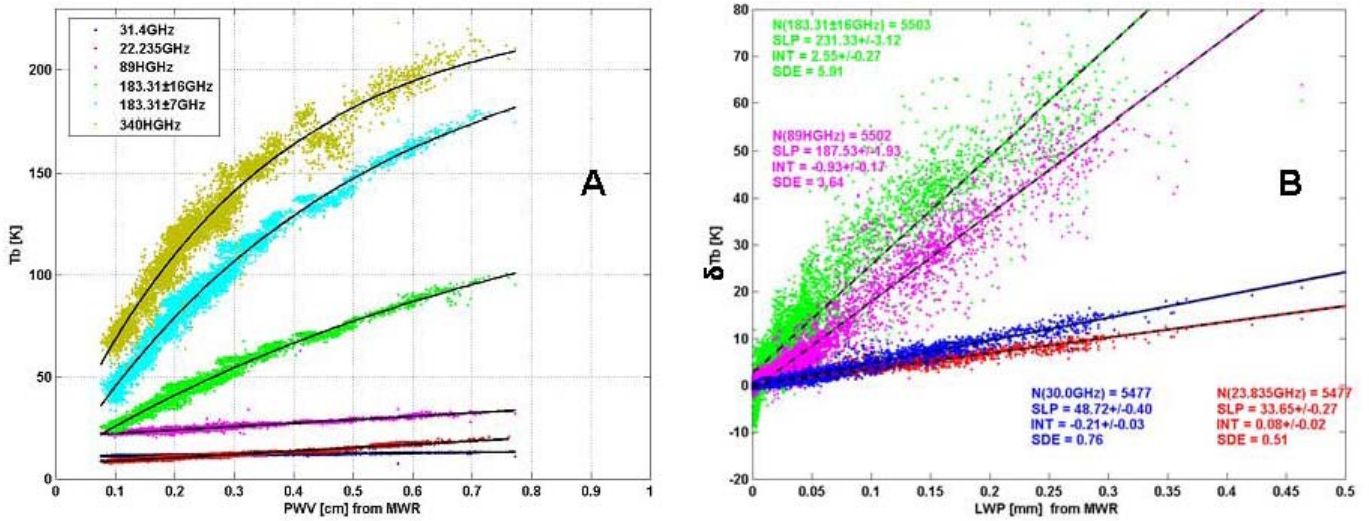
Figure 4. Measured Tb response to (A) PWV and (B) LWP for selected channels. The procedure to derive these curves is given in [2].

One of the potential benefits of the GSR is its scanning capability. By performing a complete vertical scan every two minutes, the GSR provides a set of calibrated Tb's over a ± 75° angular elevation range. Comparisons of two channels of the GSR with coincident channels of the MWRP are shown in Figure 5. Simulations based on the absorption model given in [5], and co-located Vaisala RS90 radiosondes are also shown. The simulations and the measurements agree to within ~0.5 K.
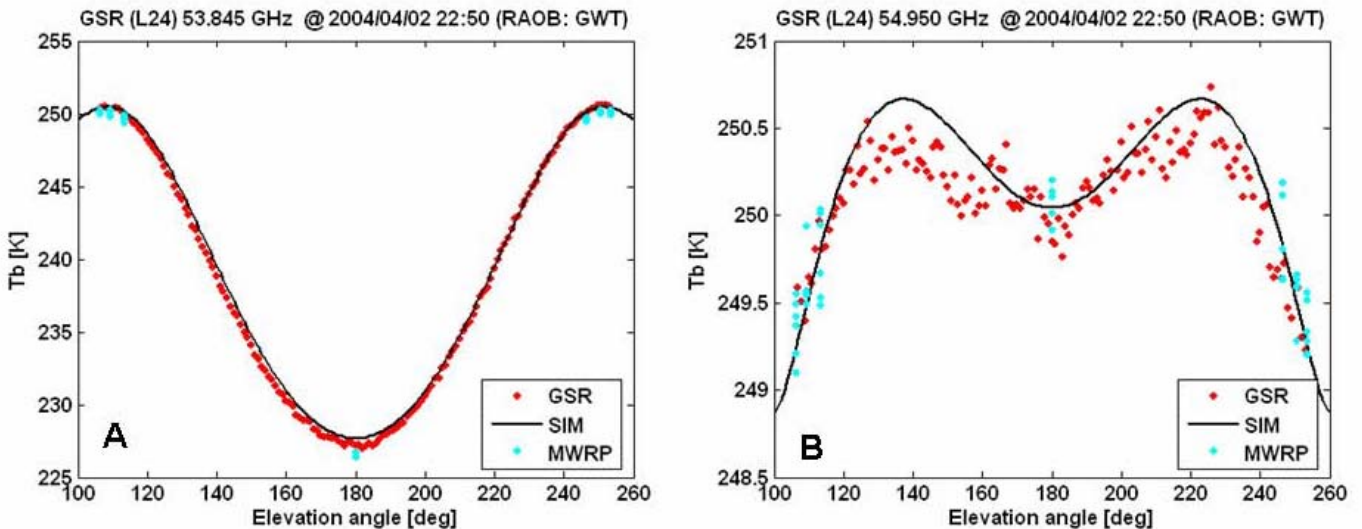
Figure 5. GSR and MWRP observations compared with radiosonde-based simulations. (A) 53.845 GHz. (B) 54.950 GHz.

In Figure 6, we show a 24-hr time series of measured and calculated data from (A) the MWR, and (B, C, and D) the GSR. Note the 1 K drop in Tb at 23.8 GHz around 91.5 Universal Time Coordinates (UTC). The corresponding gradient shown by the submillimeter-wave channels is of the order of 30 K, illustrating the enhanced sensitivity at the higher frequencies. A complete statistical analysis of the comparison between the models and measurements is under progress.
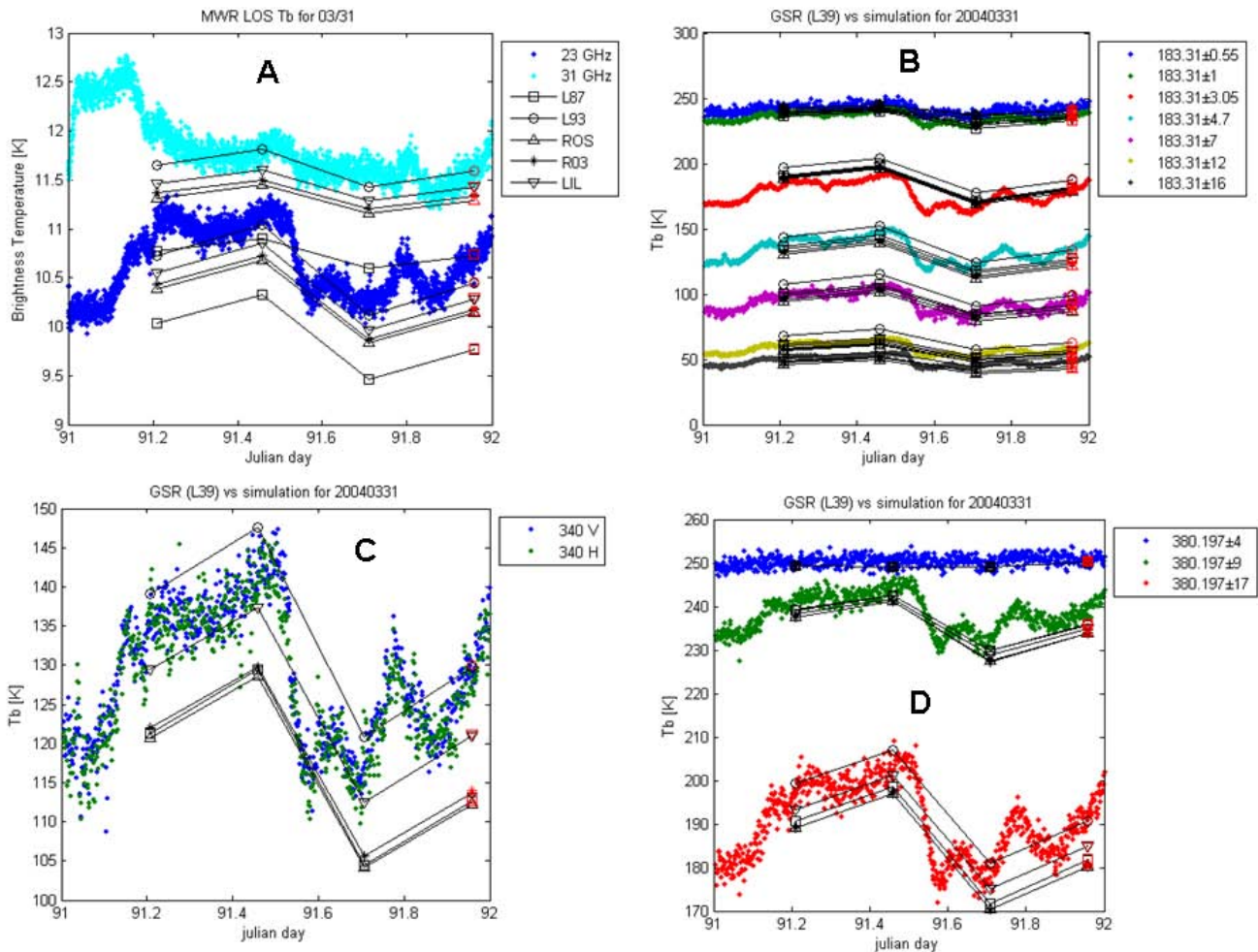
Figure 6. 24 hour time series of MWR and GSR Tbs. Note the 1 K drop at 23.8 GHz around 91.5 UTC; the corresponding gradient shown by submillimeter-wave channels is of the order of 30 K.

Radiosonde Data

In the 2004 IOP, three different humidity sensors were deployed from three separate locations near Barrow (see Figure 7). ARM Operational radiosondes were launched once-daily at 2300 UTC at the Great White (GW) site. In addition, at the ARM Duplex (DPLX) in Barrow, 2.2 km to the west of the GW, Balloon Borne Sounding System radiosondes were launched four-times daily (0500, 1100, 1700, and 2300 UTC). Data from synoptic radiosondes from the National Weather Service (NWS) (1100 and

DPLX (71.33N, 156.68W, 8m asl): RAOBS
GW (71.32N, 156.62W, 8m asl): RAOBS, MWR, MWRP, GPS
NWS (71.30N, 156.78W, 12m asl): RAOBS
d1=2.4; d2=6.1; d3=4.9 (km)
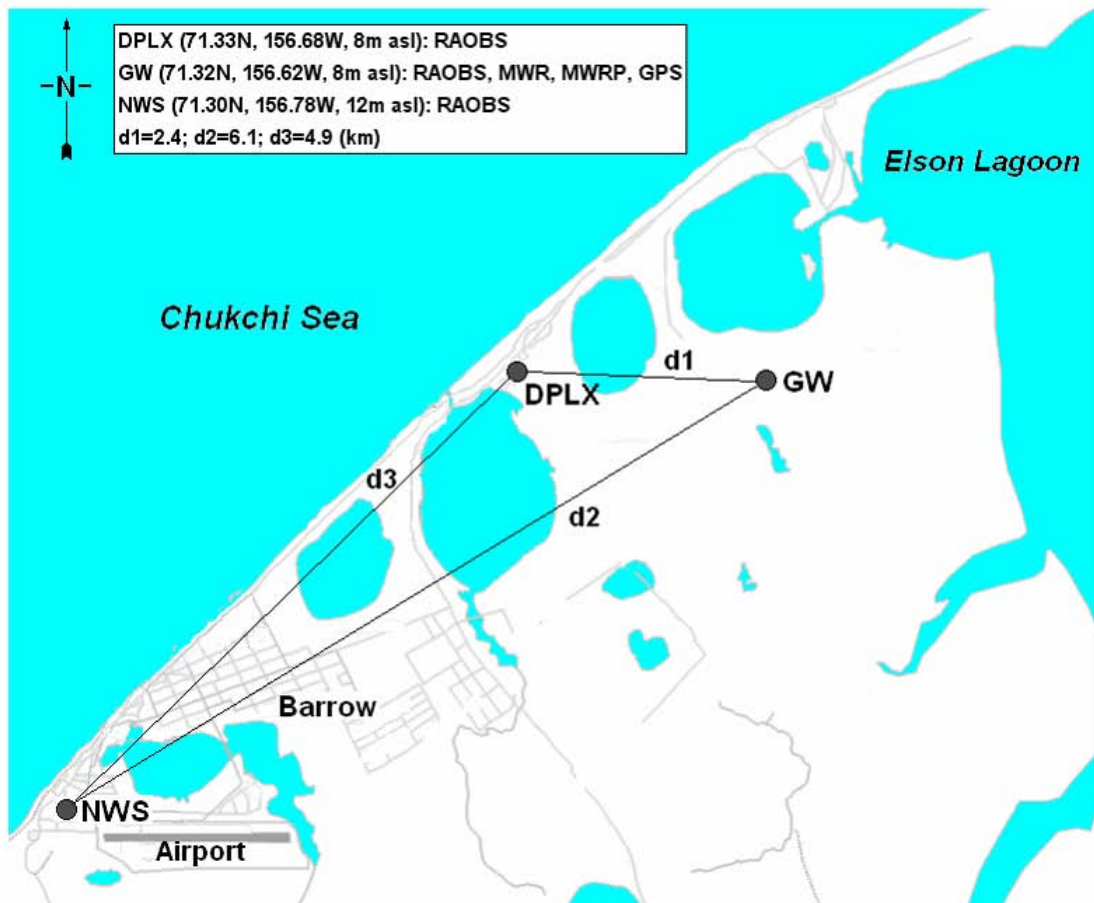
Figure 7. Map of Barrow with distance between radiosonde launch sites.

2300 UTC) were also archived. The NWS site is located in Barrow, 4.3 km to the southwest of the Great White. Finally, during clear conditions, eight dual-radiosonde launches (See Section 3c) were conducted at the ARM Duplex. This collection of almost simultaneous and nearly co-located RAOBs allowed us to compare various aspects of temperature and humidity measurements. A comprehensive analysis of the radiosonde data and subsequent analysis is contained in [4].

Radiosonde Types

VAISALA RS90

From the beginning of the experiment, radiosondes of the Vaisala RS90-A type were launched at the ARM DPLX in Barrow and at the ARM GW site. For convenience, these radiosondes will be referred to as DPLX-RS90 and GW-RS90, respectively. The RS90-A is a "PTQ-only" system, i.e., the primary measurements are pressure (P), temperature (T), and relative humidity (RH). Altitude and dew point

temperature are derived quantities in the data. The sensor for the temperature measurement is the Vaisala F-Thermocap, which consists of a capacitive wire. The sensor for the relative humidity is the Vaisala H-Humicap, a thin film capacitor with a heated twin-sensor design: two humidity sensors work in phase so that while one sensor is measuring, the other is heated to prevent ice formation. Samples were taken every 2 seconds.

Sippican VIZ-B2

During the experiment, the synoptic radiosondes launched in Barrow by the NWS were also collected. These radiosondes are Sippican VIZ-B2 type. The VIZ radiosondes were used at all NWS stations until 1995, when NWS started a process of replacement with the RS80-57H radiosondes manufactured by Vaisala. The VIZ-B2 radiosonde measure pressure, temperature, relative humidity, wind direction and wind speed every 6 seconds. Altitude and dew point temperature are derived quantities in the data. Here, these soundings will be referred to as NWS-VIZ. The sensor for the temperature measurement is a long rod thermistor, and the sensor for humidity measurements is a carbon hygristor (CH).

Sippican Mark-II with Meteolabor Snow White

During the experiment, eight successful dual-radiosonde launches were conducted at the ARM Duplex, three during the day and five during the night, in cooperation with the National Aeronautics and Space Administration. Two radiosonde packages flew on the same balloon. The first package was the ARM DPLX-RS90. The second was a radiosonde of the Sippican GPS Mark II type, operated by National Aeronautics and Space Administration, which contained a VIZ thin rod thermistor for temperature measurements and a VIZ carbon hygristor humidity sensor. The Mark II radiosonde had also attached a "Snow White" chilled mirror dew-point hygrometer, manufactured by Meteolabor AG, Switzerland. For convenience, we will refer to the Mark II humidity sensor and to the Snow White as MK2-CH and MK2-SW, respectively.

Temperature Comparisons

Figure 8 shows the temperature difference profiles between the NWS-VIZ soundings and the DPLX-RS90. The comparison is performed with the dataset divided into data taken at night at 1100 UTC (2 a.m. AST) and during the day at 2300 UTC (2 p.m. AST). Two features can be noticed. First, there is a gradient in temperature around 1000 hPa (corresponding to about 100–300 m above the surface), with the temperature over the NWS station higher than over the DPLX. The gradient in temperature is also present in the temperature comparison of NWS-VIZ and the GW-RS90 radiosondes (not shown). This phenomenon could again be explained by the presence of local heating in the town of Barrow. As was shown in Figure 7, the NWS station is in the town, the DPLX is located in the periphery of the town, and GW is the farthest site from the town.
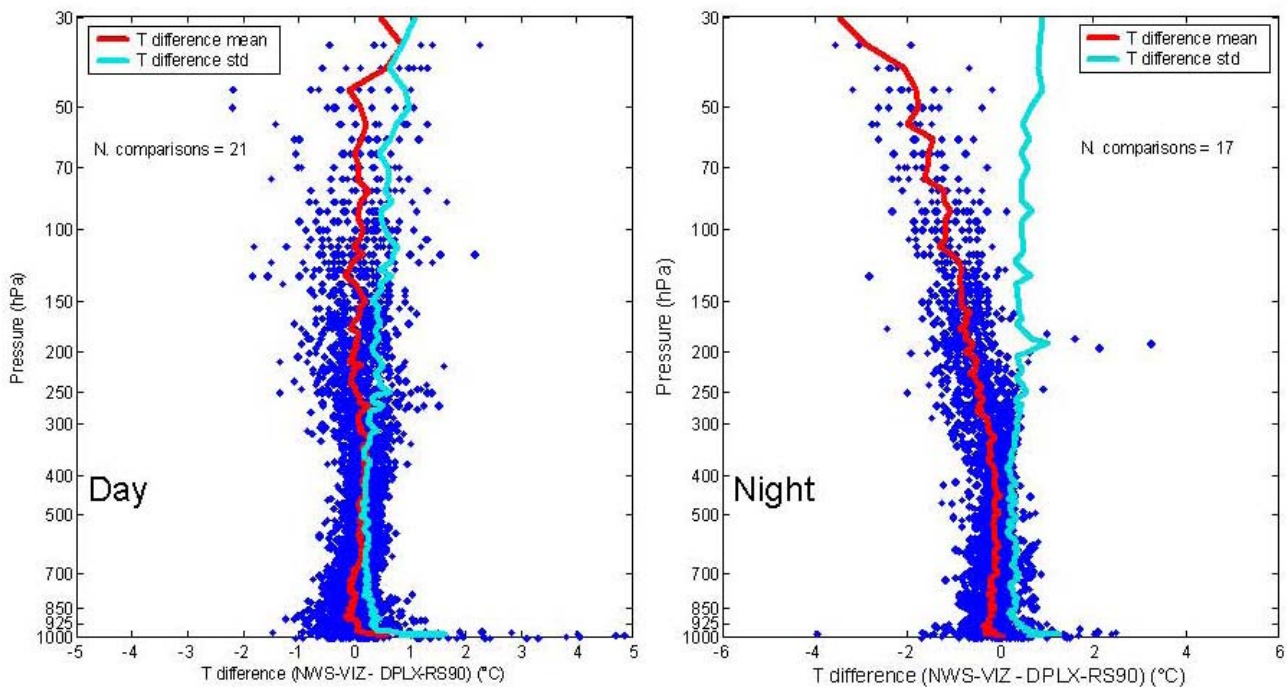
Figure 8. Comparison of temperature profile differences between VIZ vs. DPLX RS90 Radiosondes during the (A) day and (B) night. After [4].

Second, our partition indicates the presence of a negative bias up to –3.5°C at 30 hPa for pressures lower than 250 hPa, between the NWS and the DPLX temperature, during the night, and from 915 to 50 hPa, almost no bias during the day. This latter behavior was also found in the comparison between the NWS-VIZ and the GW-RS90 (not shown). Also not shown, the nighttime bias reached –5°C at 20 hPa. A possible cause is in the magnitude of the radiation correction between the two types, since NWS does not apply such correction to the VIZ-B2 sondes. All the Vaisala radiosonde temperature data were corrected automatically for radiation errors by using the most recently supplied manufacturer's correction tables. Because the NWS-VIZ thermistor is a long white-coated rod, it has a very large infrared error due to emission (emissivity 0.9), while its short-wave absorptivity is much less (~0.14). Both Vaisala sensor absorptivity and emissivity are quite small (<0.1). Therefore, the rod has a large infrared error that is especially noticeable at night when compared with Vaisala type sensors (Schmidlin et al. 1986). The error of the rod is keyed to the background radiative environment and can be different depending on location and conditions. Complete details of this analysis are contained in [4].

Relative Humidity Comparisons

Figure 9A shows how the sounding differences are manifested for a single set of measurements by all 5 sensors, and Figure 9B shows statistical comparisons of the RH measurements [4]. Since no specific difference was found in the day and night partition, the comparison is shown for the entire dataset. At 1000 hPa, the RH profiles of NWS-VIZ radiosondes are 2% lower on average with respect to the
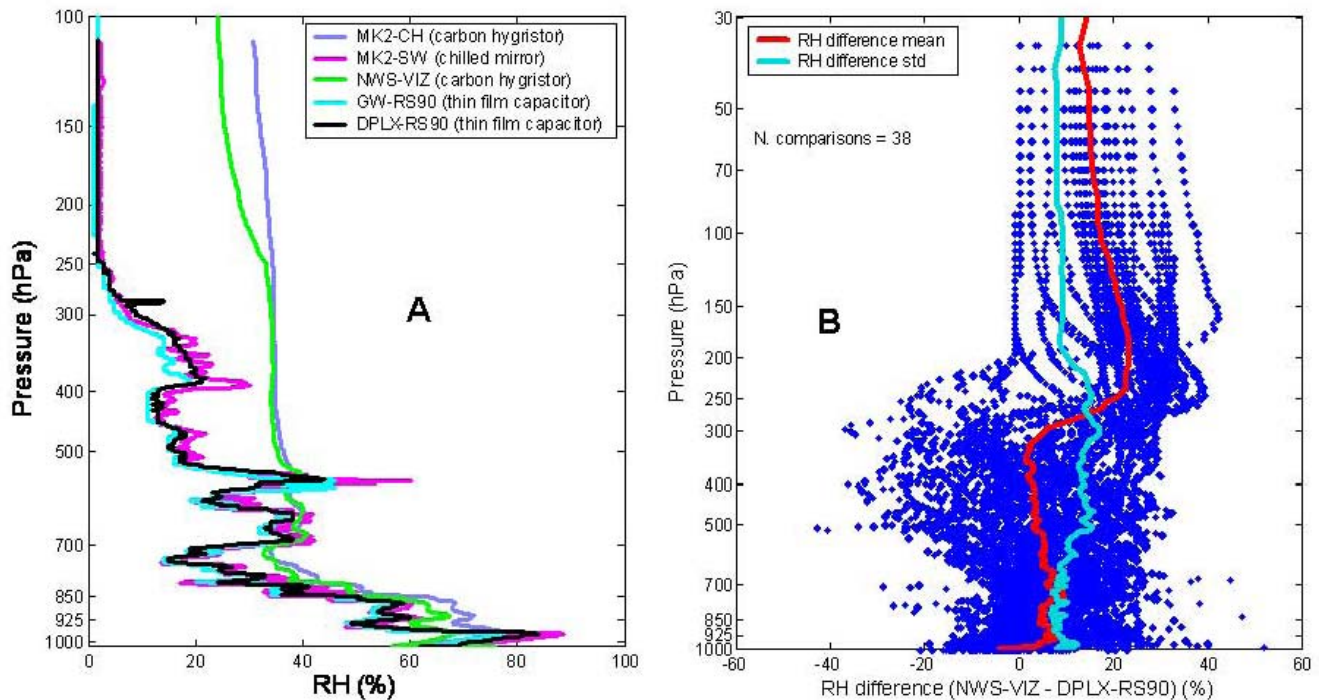
Figure 9. (A) Comparison of 5 radiosonde humidity measurements taken at the same time. (B) Comparison of NWS-VIZ with Vaisala RS90 RH soundings. (After [4]).

DPLX-RS90. At pressures lower than 925 hPa, the RH from the NWS-VIZ carbon hygristor is on the average larger than the one from the Vaisala H-Humicap at the DPLX. Above 925 hPa, the RH from the NWS-VIZ carbon hygristor is on the average larger than the one from the Vaisala H-Humicap at the DPLX. This bias increases to values as large as 23%, starting at about 250 hPa, with an average value of 17%. The average RH difference is 4% for pressures greater than 250 hPa. The average standard deviation difference for pressures greater and lower than 250 hPa is 12% and 9%, respectively. It is clear from both statistical and anecdotal profiles that significant RH discrepancies (up to ~20%) are exhibited in the upper troposphere.

Comparison with the MWRP Humidity Channels

Comparisons of PWV, as derived from the MWRP, the MWR, and the GPS with that computed by integrating the absolute humidity from soundings were performed, except for PWV less than 2 mm [4]. However visual inspections of measured and calculated Tb's at 22.235 GHz by the MWRP showed significant differences, sometimes as much as 5 K. An explanation why the PWV measurements more or less agreed between all systems, but that significant differences at 22.235 GHz existed is found by comparing weighting functions for the 5 channels. In Figure 10A we see that the response of the 30 and 26.235 GHz MWRP channels decrease with altitude, the "hinge point" channel 23.835 is almost constant with altitude, and the two frequencies closest to 22.235 GHz increase with altitude. However, on a height scale to 40 km (Figure 10 B), it is seen that the 22.235 GHz channel exhibits a factor of 10 to
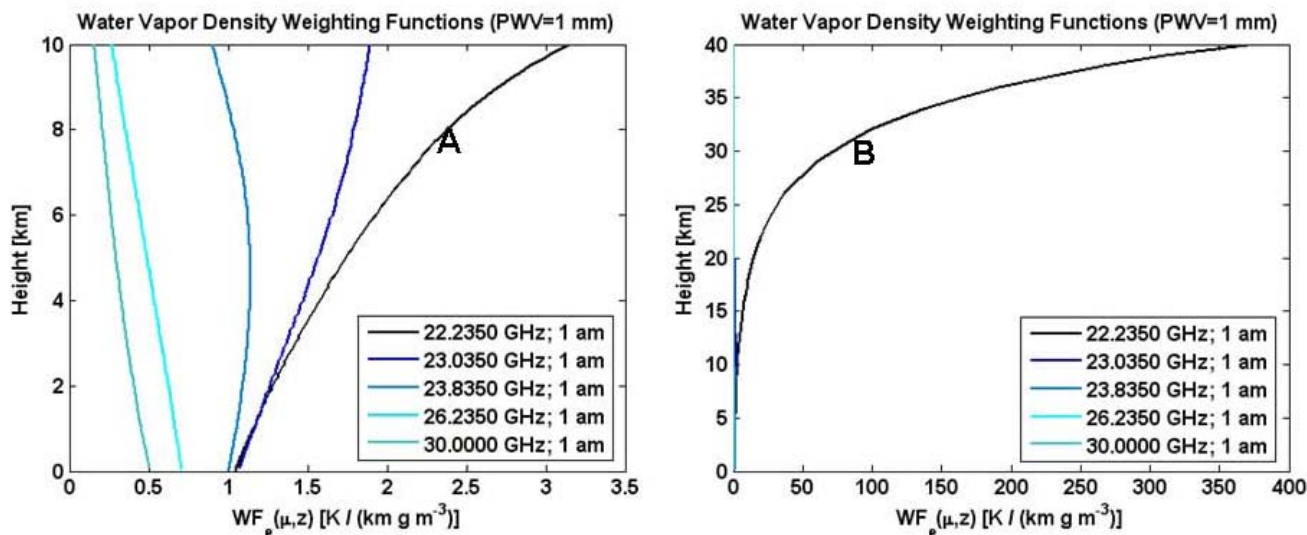
Figure 10. Water vapor weighting functions for the 5 MWRP humidity channels: (A) height to 10 km, (B) height to 40 km.

100 greater sensitivity of humidity above 15 km. The differences in response between the MWRP measurements at 22.235 GHz and the Vaisala RS90 and NWS-VIZ are shown in Figure 11. This figure demonstrates unequivocally that there is a significant problem with the NWS-VIZ upper altitude measurements.
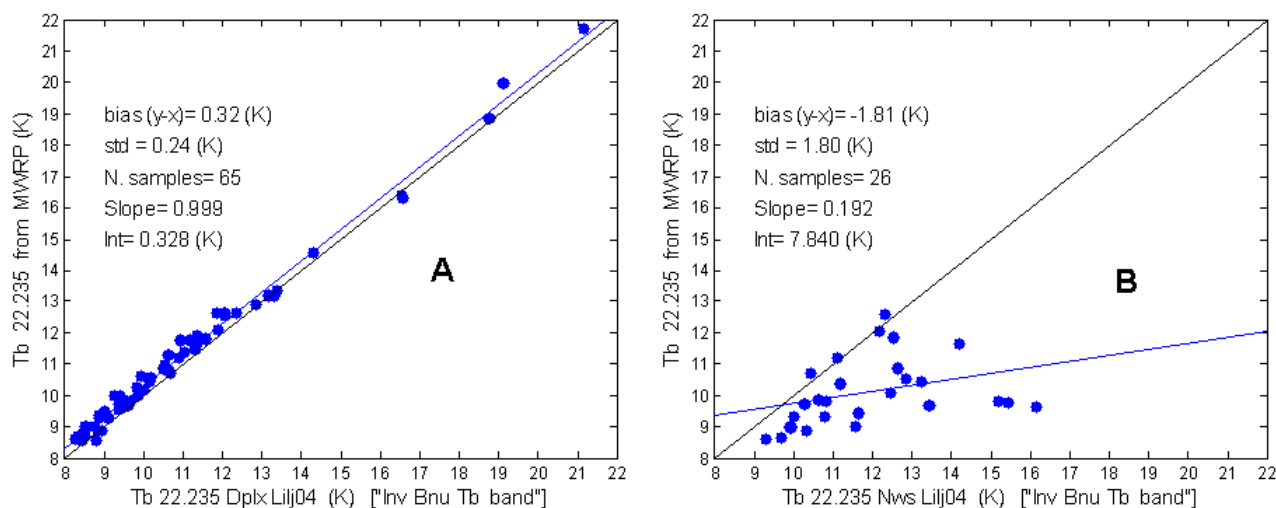
Figure 11. Comparison of Tb measured at 22.235 GHz by the MWRP with (A) calculations from the Vaisala RS90 radiosondes launched at the ARM Duplex, and (B) from the NWS-VIZ radiosondes launched in Barrow. The absorption model used is from [5].

Forward Model Studies

In Figure 12, we show results for a single GSR channel at 183.31 ± 7 GHz and two of the five models that we are evaluating. However, the results are typical and illustrate some of the uncertainties that arise from this experiment. First, we note that the results from LIL05 [5] are here much better than those of ROS98. Over a range of Tb of about 150 K, the LIL05 results are in excellent agreement exhibiting an rms discrepancy of 3.2 K. Part of the difference comes from radiosonde location as shown by the results using the DPLX radiosondes differing from those of the co-located radiosondes at the GW by an average of ~1.25 K and an rms difference of 2.1 K. We are in the process of completing the forward model studies and are using either the measured or theoretical band pass functions of the various channels, as well as an improved calibration method for the GSR channels.
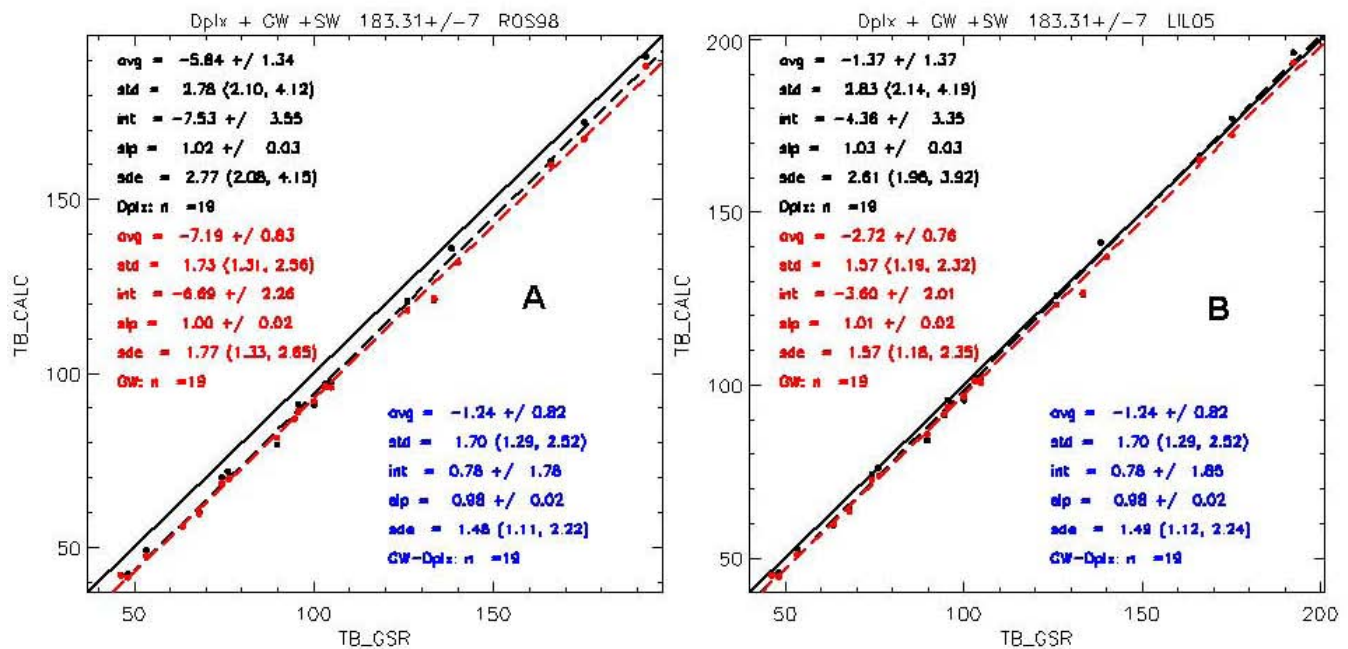
Figure 12. Comparison of calculated and measured Tbs at 183.31 ± 7 GHz from (A) ROS98 with those calculated from (B) LIL05. The black points and labels refer to calculations based on RS90 radiosondes launched from the ARM Duplex. Red points refer to RS90 radiosondes launched from the Great White, and the statistics shown in blue refer to differences for the same models and measurements, but for the radiosondes launched at the two different locations.

Conclusions and Future Work

In this paper, we have presented a summary and some of the highlights of the 2004 Arctic Winter Radiometric Experiment that was held in Barrow Alaska. A companion paper by [2] gives some of these results in greater detail. The data from the principal radiometric systems operating there (GSR, MWR, and MWRP) all showed promise for remote sensing in a cold Arctic atmospheric. In particular,

the GSR channels offer significant promise for remote sensing of PWV for amounts less than 2 mm - a region in which radiosondes, MWR, MWRP, and GPS, all have significant problems. The increased sensitivity of the channels above 89 GHz also show promise for overcoming one of the principal limitations of the MWR, i.e., low sensitivity to LWP amounts less than 50 g/m^2. One of the most significant results was the ability of the 22.235 GHz channel of the MWRP to identify erroneous upper tropospheric soundings of water vapor by the NWS-VIZ radiosondes launched at Barrow. These radiosonde data have been an important part of the US Arctic climate record. Future work includes forward model studies involving the absorption models [5, 6, 7, 8, 9] and implementing the profile retrieval method discussed in [2].

References

[1] Westwater, ER, M Klein, V Leuski, AJ Gasiewski, T Uttal, DA Hazen, D Cimini V Mattioli BL Weber, S Dowlatshahi, JA Shaw, JS Liljegren, BM Lesht, and BD Zak. 2004. "Initial results from the 2004 North Slope of Alaska arctic winter radiometric experiment." In *Proceedings of the International Geoscience and Remote Sensing Symposium (IGARSS).*

[2] Ciminil, D, ER Westwater, AJ Gasiewski, M Klein1 V Leuski1, and JC Liljegren. "Millimeter- and submillimeter-wave observations of low vapor and liquid water amounts in the arctic winter." In *Proceedings of the Sixteenth ARM Science Team Meeting*, U.S. Department of Energy.

[3] Racette, PE, ER Westwater, Y Han, AJ Gasiewski, M Klein, D Cimini, DC Jones, W Manning, EJ Kim, JR Wang, Vl Leuski, P Kiedron. 2005. "Measurement of low amounts of precipitable water vapor using ground-based millimeterwave radiometry." *Journal of Atmospheric and Oceanic Technology* 22(4)317 - 337.

[4] Mattioli, V, ER Westwater, D Cimini, JS Liljegren, BM Lesht, SI Gutman, and FJ Schmidlin. 2006. "Analysis of radiosonde and ground-based remotely sensed PWV data from the 2004 North Slope of Alaska arctic winter radiometric experiment." *Journal of Atmospheric and Oceanic Technology* (submitted 2006).

[5] Liljegren, JC, SA Boukabara, K Cady-Pereiria, and SA Clough. 2005. "The effect of the half-width of the 22-GHz water vapor line on retrievals of temperature and water vapor profiles with a 12-channel microwave radiometer." *IEEE Transactions of the Geosciences Remote Sensing* 43(5).

[6] Liebe, HJ, and DH Layton. 1987. "Millimeter wave properties of the atmosphere: Laboratory studies and propagation modeling." Nat Tech. Inf. Service, Springfield, Virginia, NTIA Rep. 87-24.

[7] Liebe, HJ, GA Hufford, and MG Cotton. 1993. "Propagation modeling of moist air and suspended water/ice particles at frequencies below 1000 GHz." In *Proceedings of the AGARD Conference* 542:3.1–3.10.

[8] Rosenkranz, PW. 1999. "Water vapor microwave continuum absorption: A comparison of measurements and models." *Radio Science* 33(4)919–928, and "Correction to 'Water vapor microwave continuum absorption: A comparison of measurements and models'." *Radio Science* 34(4)1025.

[9] Rosenkranz, PW. 2003. Private communication, August.

[10] Shupe, MD. 2005. Private communication, November.